cells

MDPI

Article

iPLA$_2$β Contributes to ER Stress-Induced Apoptosis during Myocardial Ischemia/Reperfusion Injury

Tingting Jin [1,2,†], Jun Lin [1,2,†], Yingchao Gong [1,2], Xukun Bi [1], Shasha Hu [1], Qingbo Lv [1,2], Jiaweng Chen [2], Xiaoting Li [1], Jiaqi Chen [2], Wenbin Zhang [1,*], Meihui Wang [2,*] and Guosheng Fu [1,2,*]

[1] Department of Cardiology, Sir Run Run Shaw Hospital, Zhejiang University School of Medicine, Hangzhou 310020, China; 11818361@zju.edu.cn (T.J.); 288669@zju.edu.cn (J.L.); 21818353@zju.edu.cn (Y.G.); bixukun@zju.edu.cn (X.B.); hushasha503@163.com (S.H.); lvqingbo@zju.edu.cn (Q.L.); lixiaoting26@zju.edu.cn (X.L.)

[2] Key Laboratory of Cardiovascular Intervention and Regenerative Medicine of Zhejiang Province, Sir Run Run Shaw Hospital, Zhejiang University School of Medicine, Hangzhou 310027, China; CJW19951006@163.com (J.C.); jackiechen684@gmail.com (J.C.)

* Correspondence: 3313011@zju.edu.cn (W.Z.); 3412133@zju.edu.cn (M.W.); fugs@zju.edu.cn (G.F.)

† These authors share first authorship.

Abstract: Both calcium-independent phospholipase A2 beta (iPLA$_2$β) and endoplasmic reticulum (ER) stress regulate important pathophysiological processes including inflammation, calcium homeostasis and apoptosis. However, their roles in ischemic heart disease are poorly understood. Here, we show that the expression of iPLA$_2$β is increased during myocardial ischemia/reperfusion (I/R) injury, concomitant with the induction of ER stress and the upregulation of cell death. We further show that the levels of iPLA$_2$β in serum collected from acute myocardial infarction (AMI) patients and in samples collected from both in vivo and in vitro I/R injury models are significantly elevated. Further, iPLA$_2$β knockout mice and siRNA mediated iPLA$_2$β knockdown are employed to evaluate the ER stress and cell apoptosis during I/R injury. Additionally, cell surface protein biotinylation and immunofluorescence assays are used to trace and locate iPLA$_2$β. Our data demonstrate the increase of iPLA$_2$β augments ER stress and enhances cardiomyocyte apoptosis during I/R injury in vitro and in vivo. Inhibition of iPLA$_2$β ameliorates ER stress and decreases cell death. Mechanistically, iPLA$_2$β promotes ER stress and apoptosis by translocating to ER upon myocardial I/R injury. Together, our study suggests iPLA$_2$β contributes to ER stress-induced apoptosis during myocardial I/R injury, which may serve as a potential therapeutic target against ischemic heart disease.

Keywords: iPLA$_2$β; lysophosphatidylcholine; ER stress; ischemia/reperfusion injury; apoptosis; translocation

Citation: Jin, T.; Lin, J.; Gong, Y.; Bi, X.; Hu, S.; Lv, Q.; Chen, J.; Li, X.; Chen, J.; Zhang, W.; et al. iPLA$_2$β Contributes to ER Stress-Induced Apoptosis during Myocardial Ischemia/Reperfusion Injury. *Cells* **2021**, *10*, 1446. https://doi.org/10.3390/cells10061446

Academic Editors: Antonio Rodríguez-Sinovas, Xuejun Wang, Guo-Chang Fan and Alexander E. Kalyuzhny

Received: 18 February 2021
Accepted: 7 June 2021
Published: 9 June 2021

1. Introduction

Cardiovascular disease remains the leading cause of death worldwide, imposing major burdens on our healthcare and socioeconomic systems [1]. Myocardial infarction is the irreversible injury of myocardium due to prolonged ischemia caused by coronary arteries narrowing or spasm. Myocardial ischemia/reperfusion (I/R) injury refers to circumstances wherein the ischemic myocardium resumes normal perfusion, but tissue damage is worse. Function preservation of infarcted myocardium remains a challenge for physicians [2]. Although great effort has been devoted to basic and clinical research about I/R injury, pathological mechanisms remain poorly defined [3].

I/R injury is a result of multiple factors, such as oxidative stress, intracellular Ca^{2+} overload, inflammation and metabolic derangements [4], most of which perturb the normal function of the endoplasmic reticulum (ER) and cause ER stress. ER is a subcellular organelle involved in the synthesis, maturation and transport of various proteins. Accumulation of misfolded protein in the ER leads to the unfolded protein response (UPR) to rescue

the unbalanced ER protein folding ability and rebuild ER homeostasis [5–8]. Through three discrete signaling branches, PERK, IRE1/Xbp1s and ATF6, the UPR attenuates protein translation, degrades misfolded proteins and increases the production of molecular chaperones involved in protein folding [9]. However, the UPR may promote apoptosis under prolonged stress.

Lysophosphatidylcholines (LPCs), also called lysolecithins, are a class of lipid biomolecules derived from the cleavage of phosphatidylcholine (PC) by phospholipase A2 (PLA2). LPCs accumulate in the heart during myocardial I/R injury, and some LPC species can be used as diagnostic markers of myocardial infarction [10,11]. Intracellular membrane-associated calcium-independent phospholipase A2 beta (iPLA$_2$β) catalyzes the conversion between phospholipid and fatty acids and LPC, and participates in multiple pathophysiological processes, such as apoptosis [12–15]. This enzyme, originally isolated from myocardial tissue, exhibits several specific characteristics due to its activation during ischemia, including independence of calcium, a preference for plasmalogen phospholipids containing arachidonate at the sn-2 position, and inhibition by calmodulin (CaM) and an interaction with ATP in the presence of Ca^{2+}. The cellular localization of iPLA$_2$β is tissue-specific and dynamically variable [16,17]. Additionally, iPLA$_2$β translocates to different organelles, including the plasma membrane, ER, mitochondria and nuclear membrane, and exerts different roles.

Here, we showed that the expression of iPLA$_2$β was upregulated in the heart during myocardial I/R injury, and inhibition of iPLA$_2$β reduced ER stress and myocardium damage. iPLA$_2$β may therefore represent a promising target to ameliorate cardiac damage from ischemic heart disease.

2. Materials and Methods

2.1. Chemicals and Reagents

Bromoenol lactone (BEL), thapsigargin (TG) and 4-Phenylbutyric acid(4-PBA) were acquired from Sigma-Aldrich (St. Louis, MO, USA).

2.2. Primary Neonatal Rat Ventricular Myocyte (NRVM) Isolation, Culture and Transfection

Isolation and culture of NRVMs were conducted as before [18]. In brief, hearts from 1- or 2-day-old Sprague Dawley rats were harvested (provided by the experimental animal center of Sir Run Run Shaw Hospital, affiliated with Zhejiang University). Cardiac ventricles were digested with 0.114% collagenase II (Biosharp, Shanghai, China) and 0.036% trypsin (Solarbio, Beijing, China) at 37 °C. We first pre-plated cells for 90 min to remove non-cardiomyocytes. We then cultured cardiomyocytes in Dulbecco's modified Eagle's medium (DMEM) (Cienry, Huzhou, China) supplemented with 10% fetal bovine serum (FBS) (GeminiBio, Woodland, CA, USA) and 0.1 mmol/L bromodeoxyuridine (BrdU) (Sigma, St. Louis, MO, USA). BrdU was used to reduce the proliferation of non-cardiomyocytes. After 48 h, NRVMs were cultured in DMEM without serum for another 24 h, and then they were subjected to various treatments. The Animal Welfare Ethics Committee of Sir Run Run Shaw Hospital, affiliated with Zhejiang University, approved all animal experiments. For iPLA$_2$β knockdown, NRVMs were transfected with control scrambled siRNA or siiPLA$_2$β (Sigma, St. Louis, MO, USA) mixed with Lipofectamine RNAiMax (Invitrogen, Waltham, MA, USA), based on the manufacturer's recommendations.

2.3. Simulated Ischemia/Reperfusion (sI/R) and Cell Death Assay

To simulate ischemia/reperfusion in vitro, NRVMs were washed with 1X Phosphate Buffer Saline (PBS) two times and then cultured in freshly prepared ischemic Esumi buffer [19]. Next, cells were placed in a hypoxic chamber (StemCell Technologies, Vancouver, Canada) filled with 94% N_2/5% CO_2/1% O_2 for 15 min at a rate of 20 ml/min. The chamber was sealed and kept at 37 °C for an additional 3 h. Next, we replaced the ischemic Esumi buffer with DMEM. The control group was cultured in normal DMEM. Cell death was assessed by lactate dehydrogenase (LDH) assay using Cytotoxicity LDH Assay kits according to the manufacturer's recommendations (Dojindo, Kumamoto, Japan).

2.4. Generation of iPLA$_2$β Knockout (KO) Mice

iPLA$_2$β knockout (*Pla2g6*$^{-/-}$) mice were generated by Cyagen Biosciences (Suzhou, China) with global deletion of exons 3 and 4 in the *Pla2g6* gene. iPLA$_2$β-KO mice were bred to the C57BL/6 background. Homozygous male iPLA$_2$β-KO mice of 12 to 14 weeks old were selected as the experimental group and littermate male wild-type (WT) mice were used as the control group. Genotyping primers for the *Pla2g6* null allele were: forward: 5′-GTCCACACTGGCTTGTTCCTTTAG-3′ and reverse: 5′-TGTGCCGATGTCTCTGCTAGGTAG-3′. All animal experiments were approved by the Animal Welfare Ethics Committee of Sir Run Run Shaw Hospital, affiliated with Zhejiang University.

2.5. Mouse Genotyping

The genotypes of the *Pla2g6*$^{-/-}$ mice were identified by PCR. MasterMix (2xTaq Plus) and Super DNA Marker were purchased from CoWin Biosciences (Beijing, China) (cat. No. CW2849 and CW2583). Wild-type primers were as follows: forward primer: 5′-GTCCACACTGGCTTGTTCCTTTAG-3′, reverse primer: 5′-CTCTCCTCTACACTATGACATGATC-3′, with a PCR product size of 573 bp. The mutant primers were as follows: forward primer: 5′-GTCCACACTGGCTTGTTCCTTTAG-3′, reverse primer: 5′-TGTGCCGATGTCTCTGCTAGGTAG-3′, with a PCR product size of 650 bp. PCR conditions were as follows: denaturation at 94 °C for 3 min, 94 °C for 30 s, 60 °C for 35 s and 72 °C for 35 s for 30 cycles, followed by extension at 72 °C for 5 min. Agarose gels (2%) were used for electrophoresis. Images were obtained with a Gel Doc™ XR system (Bio-Rad, Hercules, CA, USA).

2.6. Cardiac Ischemia/Reperfusion

Male mice (12–14-week-old) mice were subjected to cardiac ischemia/reperfusion (I/R) surgery as previously reported [20]. In brief, mice were anesthetized with isoflurane and placed on a heating pad to keep their body temperature between 34 °C and 37 °C. After intubation with an 18-G tracheal tube, mice were ventilated using a MiniVent mouse ventilator (tidal volume: 260 µl/stroke; ventilation rate: 100 strokes per min). An oblique incision was made from the left sternal border to observe the fourth intercostal space. Under the exposure of the left anterior descending artery, a 6–0 silk suture was tied at a position 2-mm lower than the tip of the left auricle in a loose double knot, and the thread was kept outside the chest. After 30 min of coronary occlusion, the ligation was untied in order to reestablish flow. Sham groups were subjected to only thoracotomy and closure. After 6, 24, or 72 h, animals were sacrificed for tissue collection or 2,3,5-triphenyltetrazolium chloride (TTC) staining. Infarcted area and area at risk (AAR) were quantified, and relative ratios were calculated. For tissue harvesting, left ventricles were divided into ischemic region, boundary region, and distal region. All tissues were snap-frozen in liquid nitrogen and stored at −80 °C until use.

2.7. Echocardiography

A Vevo 2100 system (MS400C probe, VisualSonics, Toronto, ON, Canada) was used to examine cardiac contractile function with conscious, mildly restrained mice. M-mode recordings were collected and analyzed to calculate left ventricular end-diastolic dimension (LVIDd) and left ventricular end-systolic dimension (LVIDs). Ventricular fractional shortening (FS%) was calculated as (LVIDd-LVIDs)/LVIDd. All measurements were performed at the papillary muscle level.

2.8. TUNEL Staining

Frozen heart sections and cultured cardiomyocytes were stained with terminal deoxynucleotidyl transferase-mediated dUTP nick-end labeling (TUNEL) using an In Situ Cell Death detection kit (Roche, Basel, Switzerland to detect apoptosis. Cryosections (5-µm thickness) were fixed with 4% paraformaldehyde and permeabilized with 0.1% Triton X-100. Cell nuclei were stained with 4′,6-diamidino-2-phenylindole (DAPI). Three fields were selected randomly for each sample to calculate the percentage of TUNEL-positive cells.

2.9. Collection of Human Blood Samples

Blood samples were collected from patients with acute myocardial infarction (AMI) within 24 h after percutaneous coronary intervention (PCI) at Sir Run Run Shaw Hospital. A control group included healthy people without AMI who visited the hospital for physical examination. Clinical diagnosis of AMI has followed WHO diagnostic criteria: 1. Symptoms of ischemic chest pain; 2. Dynamic evolution of ST-segment and T-wave (ST-T) characteristic in the electrocardiogram, or abnormal Q wave; 3. Serum myocardial enzyme spectrum increased and decreased. If two of these are satisfied, a diagnosis is made. The myocardial enzyme spectrum of patients with chest pain was measured immediately after admission, and serum cardiac troponin T (cTnT) level was much higher than 0.5ug/L, Creatine Kinase MB Isoenzyme (CK-MB) was much higher than 25IU/L. The study was conducted according to the guidelines of the Declaration of Helsinki, and approved by the Medical Ethics Committee of Sir Run Run Shaw Hospital, affiliated with Zhejiang University (20200210-113).

2.10. ELISA Assay

Blood samples clotted for 2 h at ambient temperature and were centrifuged for 15 min at 12,000 rpm 4 °C. Serum was collected and frozen at −20 °C until use. The culture medium of NRVMs was centrifuged to remove cell debris and then stored at −20 °C until use. ELISA kits for lysophosphatidylcholine (LPC) were purchased from CLOUD-CLONE CORP. (CCC, USA). LPCs in the serum of AMI patients and the culture medium of the NRVMs were then determined. ELISA kits for $iPLA_2\beta$ were purchased from GIVE (Shanghai, China) and serum $iPLA_2\beta$ concentration was evaluated according to the manufacturer's recommendations. Concentrations were calculated through standard curves using a specific curve fitting tool CurveExert 1.4. The study of human blood samples was performed according to the principles outlined in the Declaration of Helsinki. The research protocol was approved by the Medical Ethics Committee of Sir Run Run Shaw Hospital affiliated with Zhejiang University.

2.11. Immunoblotting

Cells and tissues were lysed in radioimmunoprecipitation assay (RIPA) lysis buffer (Solarbio, Beijing, China). Samples were then cleared by centrifugation (12,000 rpm, 15 min, 4 °C). Equal amount of proteins (10–20 μg) were separated by SDS-PAGE and transferred to polyvinylidene difluoride (PVDF) membranes (Millipore, Billerica, MA, USA). The following primary antibodies were used: $iPLA_2\beta$ (Santa Cruz Biotechnology, Dallas, TX, USA), GRP78 (Santa Cruz Biotechnology, Dallas, TX, USA), calnexin (Abclonal, Wuhan, China), p-IRE1α, ATF6 (Proteintech, Rosemont, IL, USA), ATF4 (Proteintech, Rosemont, IL, USA), p-PERK (Abclonal, Wuhan China), p-eIF2α (Abclonal, Wuhan, China), CHOP, cleaved caspase-3, Bax, p-CaMKII, SERCA2 (Santa Cruz Biotechnology, Dallas, TX, USA), β-actin (MultiSciences, Hangzhou, China), PERK (Abclonal, Wuhan, China), eIF2α (Abclonal, Wuhan, China), CaMKII and GAPDH (MultiSciences, Hangzhou, China). After incubation with the corresponding secondary antibodies conjugated with horseradish peroxidase (HRP) (MultiScience, Hangzhou, China), proteins were detected using a BioRad ChemiDoc MP Imaging system with enhanced chemiluminescence. All other antibodies were purchased from Cell Signaling Technology (Beverly, MA, USA).

2.12. Immunofluorescence Staining

NRVMs were subjected to sI/R, followed by fixation in 4% paraformaldehyde for 10 min. Cells were then rinsed with cold PBS three times and permeabilized with 0.5% Triton X-100 (15 min at RT). After three washes with PBS, NRVMs were blocked with 2% bovine serum albumin (BSA) in PBS (30 min at 37 °C). $iPLA_2\beta$ antibodies (1:200, Santa Cruz, sc-166616, Dallas, TX, USA) mixed with reticulum antibodies (1:200, Abclonal, A1066, Wuhan, China) were used to incubate with NRVMs overnight at 4 °C. After washing with cold PBS three times, cells were stained with Alexa Fluor-594 goat anti-mouse antibod-

ies mixed with fluorescein isothiocyanate (FITC) in 5% BSA (1 h at 4 °C). NRVMs were then counterstained with 4′, 6-diamidino-2-phenylindole (DAPI)-Fluoromount G (Southern Biotech, Birmingham, AL, USA), and images were obtained using a Leica confocal microscope. Colocalization analysis was conducted as previously reported [21].

2.13. Flow Cytometry

For quantification of cell death, NRVMs were digested with 0.05% trypsin (without EDTA) after washing with cold PBS. Cells were concentrated and suspended in 1mL PBS after neutralizing with fetal bovine serum. Annexin V-FITC and propidine iodide (PI) staining solution (Yeasen, Shanghai, China) were added, and suspensions were evaluated using flow cytometry.

2.14. RNA Isolation and Realtime PCR

Cardiac RNA was isolated using Tissue RNA Purification Plus Kits (ES Science, Shanghai, China). Approximately 10–20 mg of tissues was used for each sample. RNA from NRVMs was extracted with the Quick-RNA MicroPrep kits (ES Science, Shanghai, China). Total RNA (150–250 ng) was subjected to reverse transcription using PrimeScript RT Reagent Kits (Perfect Real Time) (TaKaRa, Tokyo, Japan). cDNA was then diluted 10-fold with ddH_2O, and quantitative real-time PCR (qRT-PCR) was performed using 2 μL cDNA and Hieff® qPCR SYBR® Green Master Mix (No Rox) (Yeasen, Shanghai, China) on a LightCycler 480 (Roche). The fold change of relative mRNA expression was calculated using the $2^{-\Delta\Delta Ct}$ method, with 18S RNA as an internal control. The primers for mouse $iPLA_2\beta$ were forward-CTGGTGCCCCTGTCTTGAAT, reverse-CGAGAACAAGTTGGTGACGC. The primers for mouse GRP78 were forward-CCTCTCTGGTGATCAGGATA, reverse-CGTGGAGAAG ATCTGAGACT. The primers for rat $iPLA_2\beta$ were forward-GCCCTGGCCATTCTACACA, reverse-CACCTCATCCTTCATACGGA. The primers for rat $iPLA_2\gamma$ were forward-CCTGAAGGAAAA GGAGTGG, reverse-CTTGTTCCTCCACCATCAAT. The primers for rat $sPLA_2$-V were forward-TCCCATCCAAGAGAACGAGTC, reverse-GTGCCACATCCACGTTTCTC. The primers for rat $cPLA_2\alpha$ were forward-AGAACACCTGGGAAGTGTGAG, reverse TGGAATAAAGCCCCTCGCTC. The primers for rat Lp-PLA_2 were forward-CGTATGCTCAACCCACCTCT, reverse-AGCCAACTCCTAGCAAAGGC. The primers for rat 18S were forward-AAACGGCTA CCACATCCAAG, reverse-CCTCCAATGGATCCTCGTTA. The primers for mouse $iPLA_2\gamma$ were forward-CATGCCGCTGGATGAATGTG, reverse-CCTTAGGACATGCGGGGTTT. The primers for mouse $cPLA_2\alpha$ were forward-AGCTTAAGGCAGGAGCTAACC, reverse-AGCATA TCGCCAAAGGTCCC. The primers for mouse $sPLA_2$-V were forward-AGAGTCTGTCCTCCT GTGTTG, reverse-TTGGGTTCTTTGTAGCCTGGT. The primers for mouse Lp-PLA_2 were forward-AGGCTGTATGCTCAACCCAC, reverse-TTTGATGTTCTGGTCACTGCAC. The primers for mouse 18S were forward-AGGGTTCGATTCCGGAGAGG, reverse-CAACTTTA ATATACGCTATTGG.

2.15. Cell Surface Protein Biotinylation and Detection

NRVMs were first subjected to sI/R. Then, cells were rinsed twice with cold PBS. EZ-link® Sulfo-NHS-LC-Biotin (Thermo Fisher Scientific, Waltham, MA, USA) at a concentration of 0.5 mg/mL was added. As a control, the same volume of PBS was used. Plates were gently shaken (30 min at 4 °C). Tris-Cl, pH 7.5 at 100 nM was used to stop biotinylation reaction. After rinsing twice with cold PBS, the cells were lysed with radioimmune precipitation buffer (RIPA). To purify surface proteins, neutravidin agarose beads were mixed with the lysate (overnight at 4 °C). The beads were then washed six times with PBS. Cell surface proteins were released by mixing with SDS-PAGE loading buffer and heating (100 °C for 5 min). Immunoblotting was then conducted to detect $iPLA_2\beta$ biotinylation. ATP1A (ATPase Na^+/K^+ transporting subunit alpha 1) was used as a cell membrane protein marker and loading control.

2.16. Assay for $[Ca^{2+}]i$ Levels

For the analysis of $[Ca^{2+}]i$ levels, cells were loaded with 5 μmol/L Fluo-4AM (Yeasen, China) at 37 °C for 30 min. The cells were digested and collected, $[Ca^{2+}]i$ levels were detected by flow cytometry.

2.17. Statistics

Data were expressed as mean ± SEM and Student's t-test was used to calculate statistical difference between two groups. Differences among multiple groups were analyzed by one-way ANOVA, followed by Tukey's test. $p < 0.05$ was considered statistically significant.

3. Results

3.1. Myocardial Ischemia/Reperfusion (I/R) Injury Induces $iPLA_2\beta$ In Vivo

Previous studies have shown that myocardial I/R injury increases the production of lysophosphatidylcholine (LPC) [22–24]. To determine whether LPC is stimulated by myocardial I/R injury in humans, we collected serum samples from 12 patients for ELISA assay. The basic demographic and clinical characteristics of the AMI patients and healthy donors are shown in Table 1. ELISA assay for LPC showed that the serum LPC level was higher in the AMI patients than the non-AMI controls (Figure 1a).

Table 1. Basic demographic and clinical characteristics of patients in two groups (n = 12).

	Non- AMI Group (n = 6)	AMI Group (n = 6)
Age (years)	54.83 ± 4.79	55.00 ± 8.72
Gender (female: male)	3:3	2:4
BMI	21.32 ± 2.32	24.77 ± 5.73
Hypertension (Yes: No)	2:4	3:3
Diabetes (Yes: No)	3:3	1:5
Smoke (Yes: No)	2:4	4:2
SBP (mmHg)	119.00 ± 11.05	121.83 ± 17.27
DBP (mmHg)	67.50 ± 10.31	77.50 ± 17.41
TG (mmol/L)	1.59 ± 1.16	1.40 ± 0.57
CHO (mmol/L)	5.13 ± 1.20	4.03 ± 1.11
HDL (mmol/L)	1.02 ± 0.15	1.04 ± 0.14
LDL (mmol/L)	2.25 ± 1.15	1.87 ± 0.62

Data are expressed as mean ± SD; AMI: acute myocardial infarction; BMI: body mass index; SBP: systolic blood pressure; DBP: diastolic blood pressure; TG: triglyceride; CHO: cholesterol; HDL: high density lipoprotein; LDL: low density lipoprotein Hypertensive patients usually take antihypertensive drugs to control their blood pressure.

Next, blood samples from 12–14-week-old mice subjected to myocardial ischemia for 30 min, followed by reperfusion for 6, 24, 72 h were collected for ELISA assay. Our results showed that LPC level was increased in mice after 24 h of reperfusion compared to the sham group (Figure 1b). LPC is generated by partial hydrolysis of phosphatidylcholines, which removes one of the fatty acid groups. This hydrolysis is generally the result of the enzymatic action of phospholipase A2 (PLA_2). Previous studies have shown that the subtypes of PLA_2, including $cPLA_2\alpha$, $sPLA_2$-V, Lp-PLA_2, $iPLA_2\beta$ and $iPLA_2\gamma$, are associated with myocardial I/R injury [25–30]. Here, we first examined the correlation between PLA_2 enzymes and I/R. We found that the mRNA level of $iPLA_2\beta$ was elevated significantly after 24 h of reperfusion, which was also consistent with the increase of LPC concentrations (Figure 1c). In contrast, the increase of other PLA_2 subtypes peaked at 6 h instead of 24 h after I/R. Next, we asked whether $iPLA_2\beta$ was also increased at the protein level upon I/R. Indeed, our $iPLA_2\beta$ ELISA data showed that serum levels of $iPLA_2\beta$ in the AMI patients were significantly higher than those in the non-AMI patients (Figure 1d). Consistently, the protein level of $iPLA_2\beta$ in mouse hearts underwent I/R was also dramatically increased (Figure 1e). Taken together, these data indicate that myocardial I/R injury induces $iPLA_2\beta$ expression in the heart.

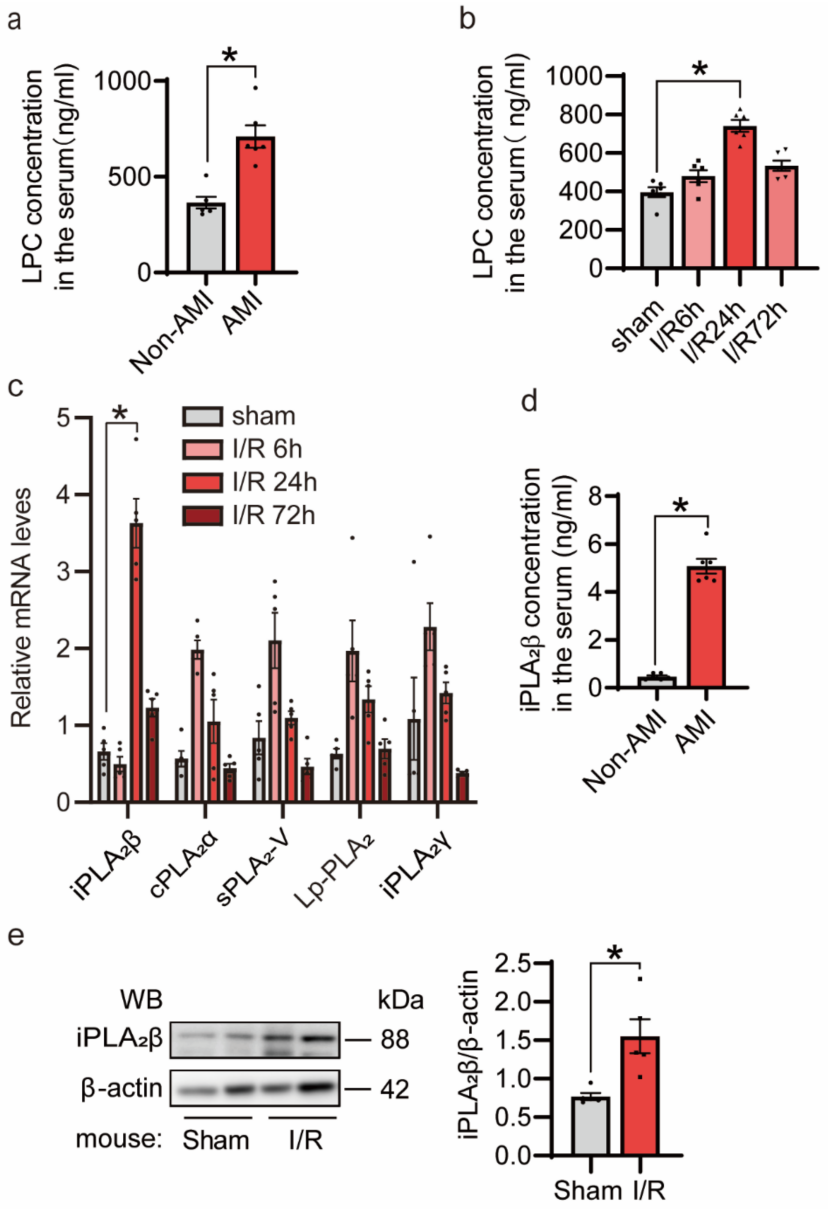

Figure 1. The elevated expression of iPLA$_2$β during myocardial ischemia/reperfusion (I/R). (**a**) Lysophosphatidylcholine (LPC) was increased in the sera of the acute myocardial infarction (AMI) patients. Twelve serum samples were collected, six of which were in the AMI group. LPC ELISA was performed to detect the LPC concentration in serum. (**b**) Upregulation of LPC in mouse sera after I/R injury. Mice at 12–14 weeks of age were subjected to myocardial ischemia for 30 min, followed by reperfusion for 6, 24, 72 h. Serum samples were collected, and LPC ELISA was performed to detect the LPC concentration. n = 6 per group. (**c**) The mRNA level of phospholipase A2 in mouse hearts upon myocardial I/R was detected. Quantitative RT PCR (qRT-PCR) was conducted to measure mRNA level changes, with 18S as an internal control. n = 5 per group. (**d**) iPLA$_2$β was upregulated in the sera of the AMI patients. iPLA$_2$β ELISA was performed to detect the iPLA$_2$β concentration. (**e**) The expression of iPLA$_2$β in mouse hearts was increased after I/R. Mice were subjected to myocardial ischemia for 30 min, followed by 24 h of reperfusion. Immunoblot analysis was performed for iPLA$_2$β. β-actin was used as a loading control. n = 5 per group. Data are represented as mean ± SEM. All experiments were independently replicated in triplicate. * $p < 0.05$.

3.2. sI/R Induced iPLA$_2$β In Vitro

We treated NRVMs using the Esumi ischemic buffer, and incubated the cells in a 94% N_2/5% CO_2/1% O_2 hypoxic chamber for 3 h. Then, the buffer was replaced with a normal medium. We next determined cardiomyocyte death by assessing LDH release. We found that sI/R induced a time-dependent increase of cardiomyocyte death (Figure 2a). We found that, consistent with the elevated LDH release, NRVMs subjected to simulated 3-h ischemia/3-h reperfusion (sI/R) showed a significant increase of iPLA$_2$β expression at both mRNA and protein levels (Figure 2b,c). In contrast, the mRNA levels of other types of PLA$_2$, including cPLA$_2$α, sPLA$_2$-V, Lp-PLA$_2$ and iPLA$_2$γ, had no significant changes (Figure 2b). Besides, LPC concentrations were also upregulated in both supernatants and intracellular extracts (Figure 2d).Following sI/R, we observed that GRP78, an ER stress marker, was increased at both mRNA and protein levels (Supplementary Figure S1a,b). Moreover, NRVMs subjected to sI/R showed an increase of the spliced form of XBP1 mRNA (Supplementary Figure S1c). In summary, these findings suggest that sI/R leads to upregulation of iPLA$_2$β and induction of the UPR.

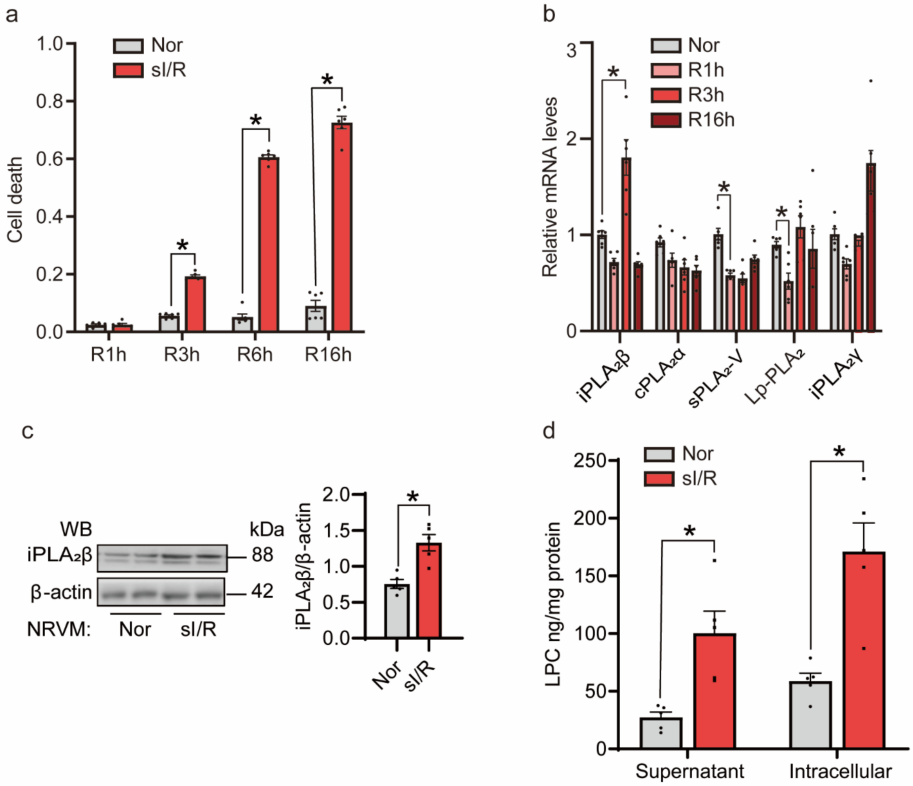

Figure 2. Simulated ischemia/reperfusion (sI/R) induces iPLA$_2$β upregulation in neonatal rat ventricular myocytes (NRVMs). (**a**) sI/R caused significant cell death. NRVMs were subjected to 3 h of ischemia followed by 3, 6, 16 h of reperfusion. Lactate dehydrogenase (LDH) was determined in culture medium and in cell lysates, respectively. Relative cell death was calculated based on the ratio of released LDH in the medium. n = 6 per group. (**b**) sI/R led to strong induction of phospholipase A2 at the mRNA level. NRVMs were subjected to ischemia for 3 h, followed by different times of reperfusion. qRT-PCR was conducted to measure mRNA changes with 18S as an internal control. n = 6 per group. (**c**) sI/R induced the expression of iPLA$_2$β at the protein level. Immunoblotting showed that iPLA$_2$β was significantly increased at the protein level (left). β-actin was used as a loading control. Quantification is shown on the right. n = 5 per group. (**d**) Lysophosphatidylcholine (LPC) was increased during sI/R. NRVMs were subjected to 3 h of ischemia and 3 h of reperfusion. LPC ELISAs were performed to detect LPC concentrations in culture medium and in cell lysates. Relative LPC concentration in cell lysates was normalized based on total cellular protein concentrations. n = 5 per group. Data are represented as mean ± SEM. All experiments were independently replicated in triplicate. * $p < 0.05$.

3.3. Knockout of iPLA$_2$β Alleviated Heart I/R Injury

To explore the role of iPLA$_2$β in vivo, we generated a *Pla2g6* (the gene encoding iPLA$_2$β) knockout (KO) mouse model (C57BL/6N) by CRISPR/Cas9-mediated genome engineering (Figure 3a). Positive mice were identified by PCR screening, and the size of the PCR products of *Pla2g6*$^{-/-}$ mice was 650 bp, whereas PCR products for the wild-type (WT, *Pla2g6*$^{+/+}$) mice were 573 bp. Mice designated #1–8 were homozygous *Pla2g6*$^{-/-}$ mice (Figure 3b), and mice designated #9–13 were homozygous *Pla2g6*$^{+/+}$ mice. To confirm the knockout of *Pla2g6*, we performed qRT-PCR and Western blotting. iPLA$_2$β-KO mice showed significantly lower iPLA$_2$β expression at both mRNA level and protein levels (Figure 3c,d). Furthermore, WT and *Pla2g6*$^{-/-}$ mice had similar body weights (Supplementary Figure S2a), heart rates (Supplementary Figure S2b), ventricular sizes and contractile functions (Supplementary Figure S2c) at baseline. Next, 30-min of myocardial ischemia and 24-h of reperfusion were performed with 12–14-week-old WT control mice and KO mice. We used TTC staining to identify and quantify damaged tissue areas (Figure 3e). The relative ratios of infarct area to area at risk (AAR) of the WT and KO hearts were calculated and compared. iPLA$_2$β deletion led to a significantly smaller infarct size (Figure 3f). In addition, there was no significant difference in the relative ratio of AAR to the left ventricle between control group and KO group, suggesting that I/R surgery was similarly conducted between groups. Moreover, echocardiographic analysis showed iPLA$_2$β deficiency resulted in improved systolic and diastolic function 24 h after I/R surgery (Table 2), which indicates that knockout of iPLA$_2$β preserves cardiac performance in respond to I/R injury. Furthermore, heart sections stained with TUNEL showed less myocardial apoptosis in iPLA$_2$β KO mice than control littermates (Figure 3g). Taken together, our data indicate that knockout of iPLA$_2$β protects the heart against I/R injury.

3.4. Inhibition of iPLA$_2$β Ameliorates NRVMs Death Triggered by sI/R In Vitro

To investigate the role of iPLA$_2$β in I/R in vitro, we adopted an inhibitor-based approach. First, after 3 h of ischemia, we inhibited iPLA$_2$β in NRVMs with 15 μM bromoenol lactone (BEL) for 15 min, which is a potent and irreversible inhibitor of iPLA$_2$β [31]. DMSO was used as a negative control. Our results showed that inhibition of iPLA$_2$β significantly reduced cell death caused by sI/R (Figure 4a). LPC ELISAs verified that BEL pretreatment reduced sI/R induced supernatant and intracellular LPC release, which was mainly due to the reduced activity of iPLA$_2$β (Figure 4b). Additionally, the decreased number of TUNEL-positive cells in the BEL-treated group confirmed that the inhibition of iPLA$_2$β protected NRVMs from the sI/R-induced cell death (Figure 4c,d). Recent studies have shown that BEL inhibits other key enzymes in phospholipid metabolism as well [31]. To further test the function of iPLA$_2$β in sI/R injury directly, we transfected NRVMs with siiPLA$_2$β to knock down iPLA$_2$β. SiiPLA$_2$β efficiently decreased target gene expression at both protein and mRNA levels (Figure 4e,f). Knockdown of iPLA$_2$β modestly but significantly decreased cell death, as shown by an LDH release assay and the LPC concentration measurement (Figure 4g,h). Furthermore, knockdown of iPLA$_2$β mitigated NRVM apoptosis caused by sI/R as shown by TUNEL assays (Figure 4i). Collectively, these results demonstrate that inhibition of iPLA$_2$β protects cardiomyocytes from sI/R injury in vitro.

Table 2. Echocardiographic measurements for iPLA$_2$β-KO and WT mice at 24 hours after I/R operation.

Parameter	WT I/R (n = 5)	KO I/R (n = 5)
IVS (mm)	1.00 ± 0.17	0.85 ± 0.96
LVPWs (mm)	1.08 ± 0.14	1.07 ± 0.22
LVIDd (mm)	3.65 ± 0.26	3.05 ± 0.41 *
LVIDs (mm)	3.22 ± 0.26	2.40 ± 0.37 *
FS (%)	11.79 ± 2.69	21.46 ± 2.26 *
EF (%)	26.02 ± 5.54	44.91 ± 4.26 *

IVS, interventricular septum thickness; LVPW, left ventricular posterior wall thickness; LVIDd, left ventricular end-diastolic dimension; LVIDs, left ventricular end- systolic dimension; FS, fractional shortening; EF, ejection fraction. * $p < 0.05$ versus WT I/R group.

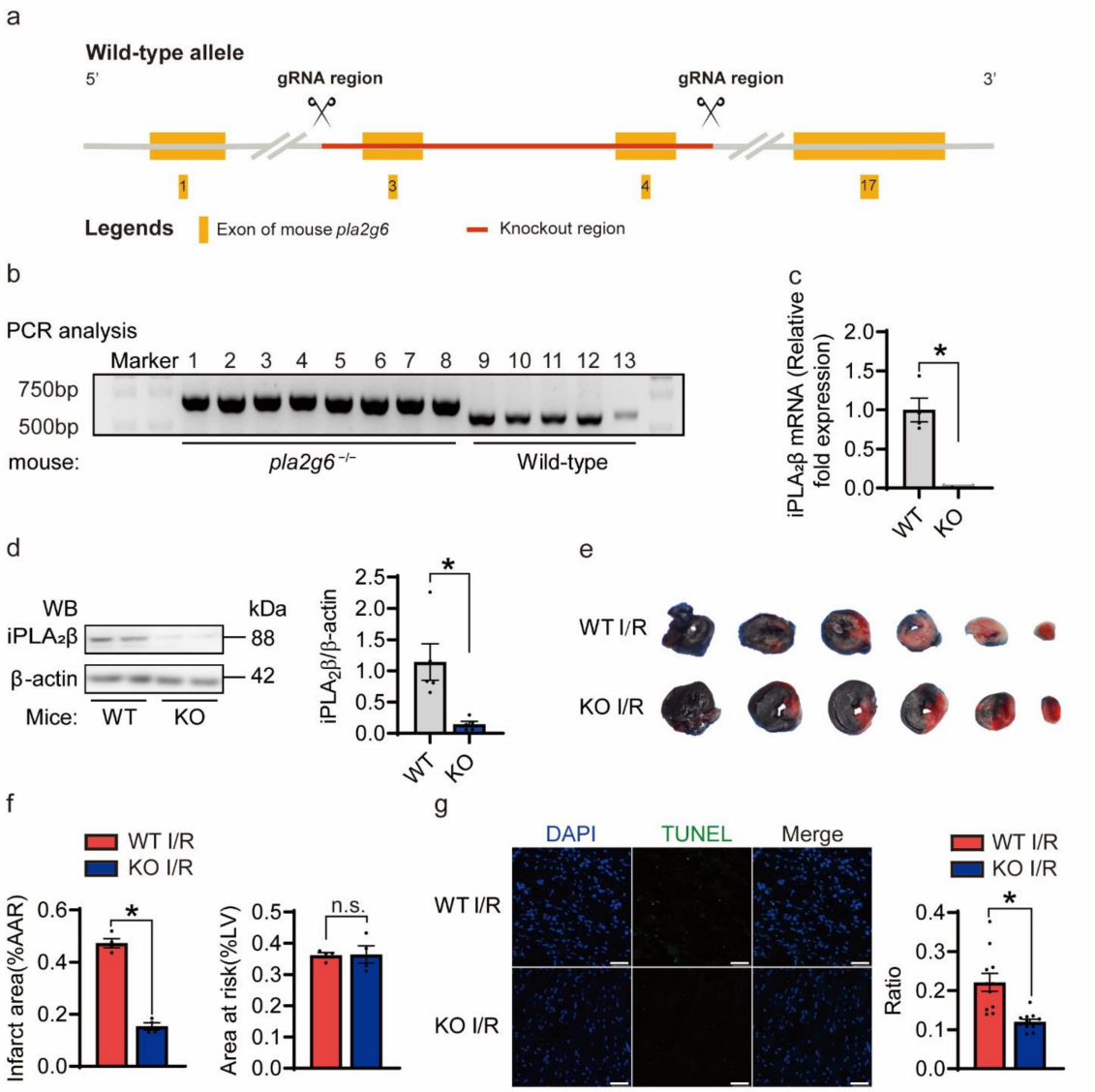

Figure 3. Knockout of iPLA$_2$β protects the heart from I/R injury. (**a**) Overview of the targeting strategy to create a *Pla2g6*$^{-/-}$ mouse model (C57BL/6N) by CRISPR/Cas9-mediated genome engineering. (**b**) Knockout (KO) mice were genotyped by agarose gel electrophoresis. The size of the PCR product of *Pla2g6*$^{-/-}$ mice was 650 bp, whereas the PCR product of the wild-type (WT, *Pla2g6*$^{+/+}$) mice was 573 bp. (**c**) Absence of iPLA$_2$β mRNA in KO mice. Total RNA was isolated from ventricular tissues of WT and iPLA$_2$β KO mice, respectively. Real-time PCR was conducted to assess iPLA$_2$β at the mRNA level. n = 4–5 for each group. (**d**) Confirmation of iPLA$_2$β deletion in iPLA$_2$β-KO mice. Total proteins were extracted from the ventricular tissues of wild-type (WT) and iPLA$_2$β-KO mice. Western blotting was conducted to assess iPLA$_2$β at protein level. n = 5 for each group. (**e**,**f**) Knockout of iPLA$_2$β protected the heart from I/R injury. WT and iPLA$_2$β-KO mice at 12–14 weeks of age were subjected to myocardial ischemia for 30 min, followed by 24 h of reperfusion. Then, 2,3,5-triphenyltetrazolium chloride (TTC) staining was conducted to detect and quantify the injured cardiac tissue. The white region depicts the ischemic infarct zone; the pink/red area is the border zone; and the blue region represents the remote zone. The relative ratio of the infarct region (IF) to the area at risk (AAR, ischemic and border) was compared between WT and iPLA$_2$β-KO mice. The relative ratio of AAR to the left ventricle did not differ between WT and KO groups, suggesting that I/R surgery was performed similarly across genotypes. n = 4 per group. (**g**) Representative photographs of heart sections stained with terminal-deoxynucleotidyl transferase-mediated dUTP nick end labeling (TUNEL) from WT and KO mice after myocardial I/R (left). Scale bar = 25 μm. Quantification is shown on the right. n = 10–11 per group. Data are represented as mean ± SEM. All experiments were independently replicated in triplicate. * $p < 0.05$.

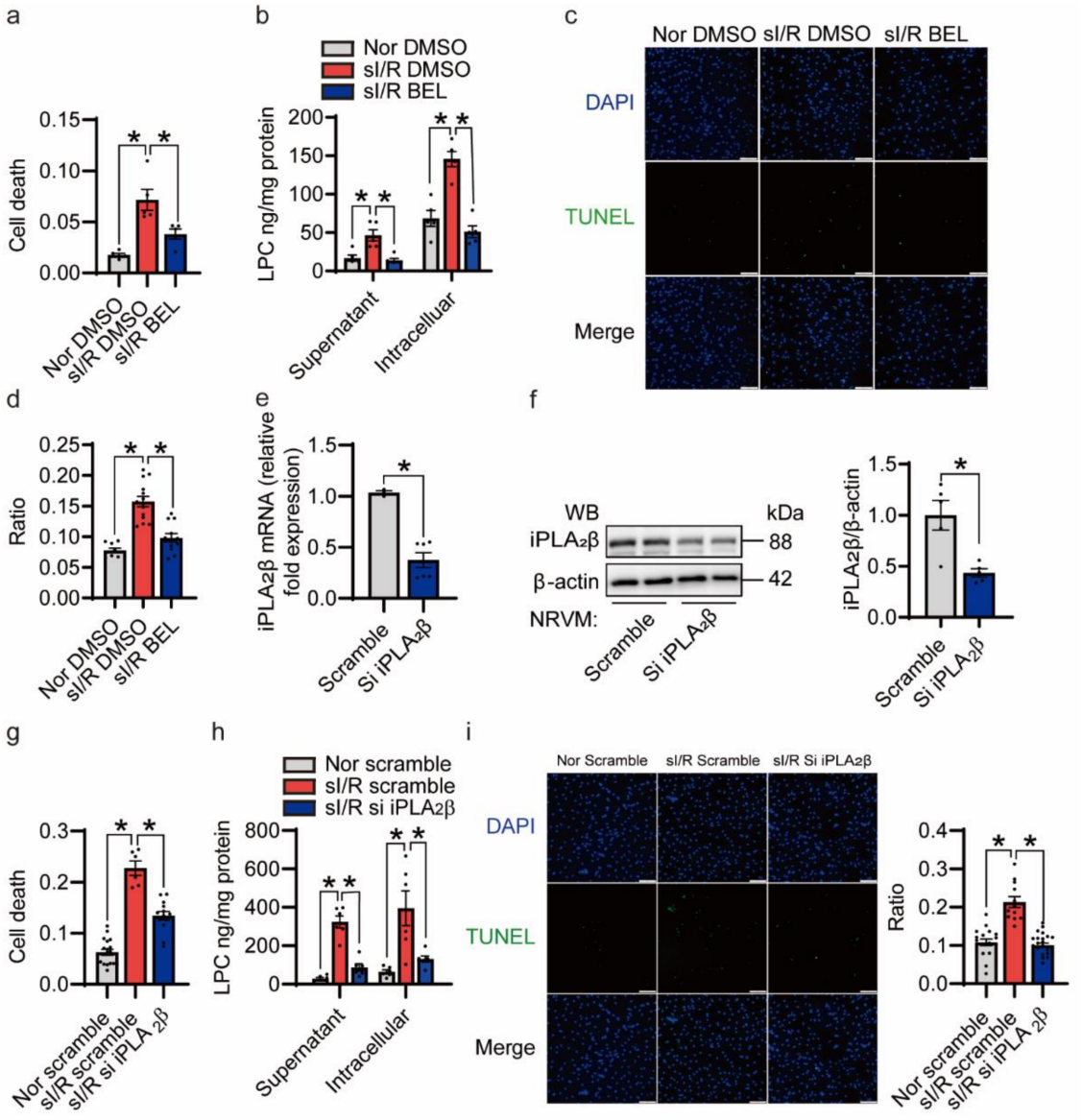

Figure 4. Inhibition of iPLA$_2$β by bromoenol lactone (BEL) or knockdown of iPLA$_2$β protects NRVMs from sI/R-induced cell death. (**a**) Inhibition of iPLA$_2$β blunts sI/R-induced cell death. NRVMs were subjected to ischemia for 3 h and then pretreated with 15 μM BEL for 15 min followed by 3 h of reperfusion. LDH levels were measured to determine relative cell death. n = 5 per group. (**b**) Inhibition of iPLA$_2$β decreased sI/R-induced LPC release. After 3 h of ischemia, NRVMs were treated with BEL, followed by reperfusion for 3 h. Relative LPC concentrations were determined with LPC ELISA kits. n = 5 per group. (**c**) Inhibition of iPLA$_2$β extenuated sI/R-induced cell apoptosis as determined by terminal-deoxynucleotidyl transferase-mediated dUTP nick end labeling (TUNEL)-positive cardiac myocytes. Apoptotic nuclei were identified by TUNEL staining (green), and total nuclei were identified by 4′,6-diamidino-2-phenylindole (DAPI) counterstaining (blue). Representative photomicrographs are shown. Scale bar = 20 μm. (**d**) Quantitative analysis of TUNEL-positive cells under the normoxic or sI/R condition. n = 6–14 per group. (**e**) The relative gene expression of iPLA$_2$β decreased in the siiPLA$_2$β-transfected NRVMs. qRT-PCR was conducted to examine mRNA level changes with 18S as an internal control. n = 3–6 per group. (**f**) Immunoblot analysis for iPLA$_2$β. β-actin was used as a loading control. n = 5 per group. (**g**) Knockdown of iPLA$_2$β attenuated sI/R-induced cell death. LDH levels were measured to determine relative cell death. n = 6–16 per group. (**h**) Knockdown of iPLA$_2$β decreased sI/R-induced LPC release. After transfection with siiPLA$_2$β, NRVMs were subjected to 3 h of ischemia and 3 h of reperfusion. Relative LPC concentrations were examined with LPC ELISA kits. n = 6 per group. (**i**) Knockdown of iPLA$_2$β attenuated sI/R-induced cell apoptosis as determined by TUNEL-positive cardiac myocytes. Representative photomicrographs are shown on the left. Scale bar = 20 μm. Quantification is shown on the right. n = 11–18 per group. Data are represented as mean ± SEM. All experiments were independently replicated in triplicate. * $p < 0.05$.

3.5. The Reduction of I/R Injury Is Mainly Achieved by Reducing Apoptosis

Previous work suggests that apoptosis is involved in myocardial I/R injury [32]. Since prolonged ER stress leads to apoptosis, we hypothesized that the inhibition of iPLA$_2$β might alleviate I/R injury caused-myocardial damage by reducing apoptosis. Indeed, flow cytometric analysis showed that the inhibition of iPLA$_2$β protected NRVMs from sI/R injury, mainly by decreasing Annexin V+/PI+-positive apoptotic cells (Figure 5a,b). We observed that the expression of CHOP was markedly reduced in the BEL-pretreated and siiPLA$_2$β-transfected NRVMs under the sI/R condition, respectively (Figure 5c,d). Moreover, the expression of CHOP in iPLA$_2$β-KO mouse hearts after I/R injury was downregulated compared to that in WT mouse hearts (Figure 5e). Additionally, there was no significant difference of CHOP expression at baseline between WT and iPLA$_2$β-KO mice (Supplementary Figure S3a).

3.6. iPLA$_2$β Translocation to the ER Aggravates ER Stress-Induced Apoptosis during I/R

The function of iPLA$_2$β is influenced by its organelle localization, which is regulated by the intracellular environment [16]. To determine the localization of iPLA$_2$β in cardiomyocyte upon I/R injury, a biotinylation experiment for cell surface proteins was conducted. sI/R did not increase the cell membrane localization of iPLA$_2$β, which actually showed a trend of decrease (Figure 6a). Immunofluorescence was next used to investigate whether iPLA$_2$β was present on the ER membrane. We found that colocalization of iPLA$_2$β and an ER marker calreticulin was significantly increased during sI/R. In contrast, iPLA$_2$β inhibition significantly disrupted iPLA$_2$β and ER colocalization (Figure 6b,c). The upregulation of ER stress markers, apoptotic markers and Ca^{2+} regulated related proteins induced by sI/R was decreased by the inhibition of iPLA$_2$β in vitro and in vivo (Figure 6d,e). Quantification of these blots were shown (Supplementary Figure S4a,b). However, significant differences were not observed in the other two UPR marker proteins, ATF6 and IRE1α (Supplementary Figure S5a,b). When NRVMs were subjected to 0.5 μM thapsigargin (TG), an ER stress activator, for 6 h, we also found that colocalization of iPLA$_2$β with ER was significantly increased under ER stress condition (Supplementary Figure S5d). Inhibition of iPLA$_2$β reduced intracellular Ca^{2+} during sI/R (Figure 6f,g). Moreover, inhibition of ER stress by 5 mM 4-phenylbutyric acid (4-PBA) for 30 min ameliorated cardiomyocyte death caused by sI/R (Supplementary Figure S5c). Collectively, these findings suggest that I/R induces iPLA$_2$β expression and promotes its translocation to the ER, which leads to unbalanced lipid metabolism homeostasis, aggravates calcium overload, triggers ER stress and eventually causes cardiomyocyte apoptosis.

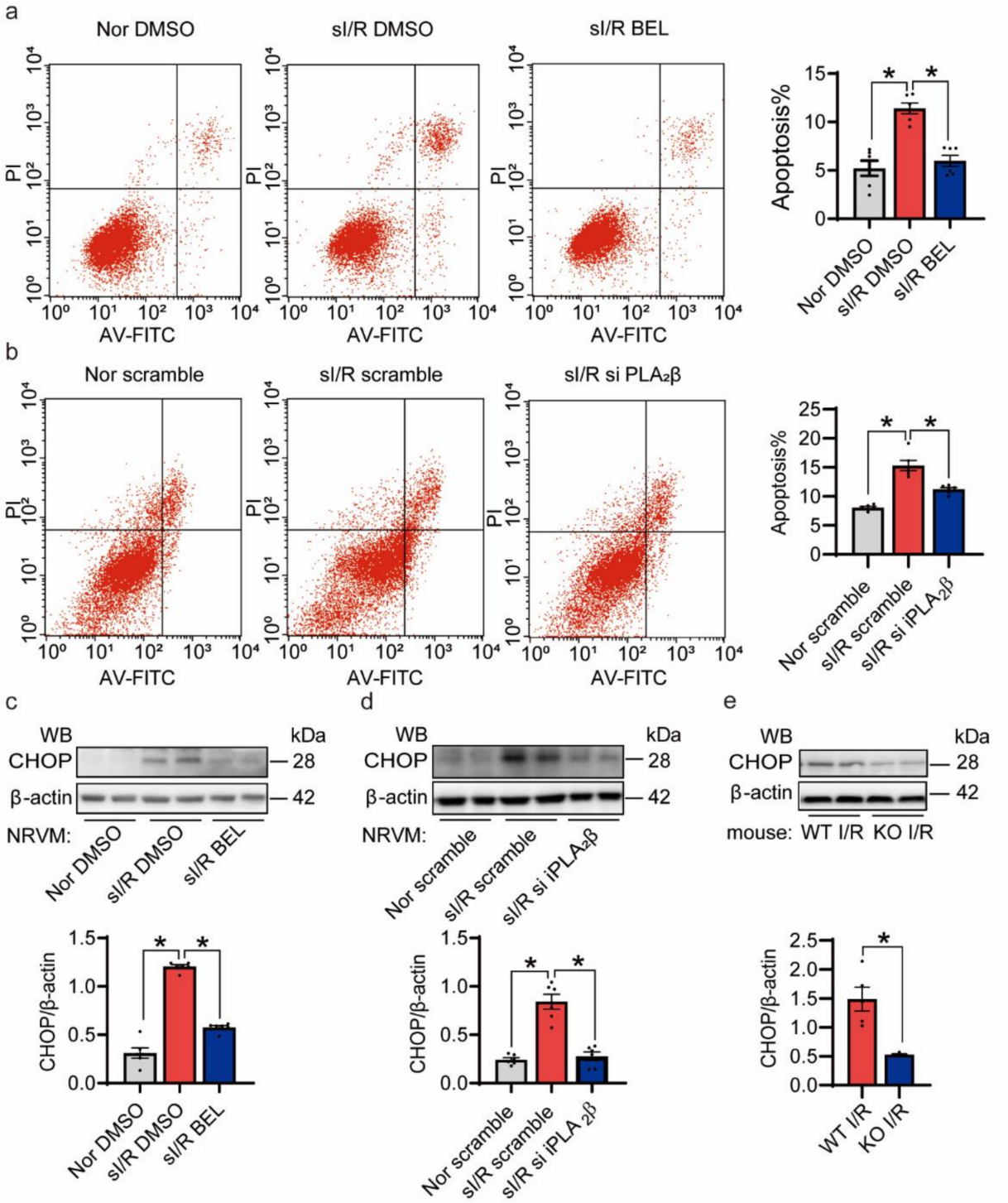

Figure 5. Inhibition of iPLA$_2$β alleviates I/R injury by reducing apoptosis. (**a**) Suppression of iPLA$_2$β by BEL conferred significant protection against I/R-induced cell death as determined by flow cytometry of Annexin V- and PI-positive cells. A representative histogram is shown. Quantification is shown on the right. $n = 6$ per group. (**b**) Knockdown of iPLA$_2$β protected NRVMs against I/R-induced cell death as determined by flow cytometry of Annexin V- and PI-positive cells. A representative histogram is shown. Quantification is shown on the right. $n = 6$ per group. (**c**) The expression of CHOP was detected and quantified by Western blotting. $n = 6$ per group. (**d**) The expression of CHOP was reduced by transfection with siiPLA$_2$β. $n = 6$ per group. (**e**) CHOP expression in the iPLA$_2$β-KO mouse heart was reduced upon I/R injury. β-actin was used as a loading control. $n = 5$ per group. Data are represented as mean ± SEM. All experiments were independently replicated in triplicate. * $p < 0.05$.

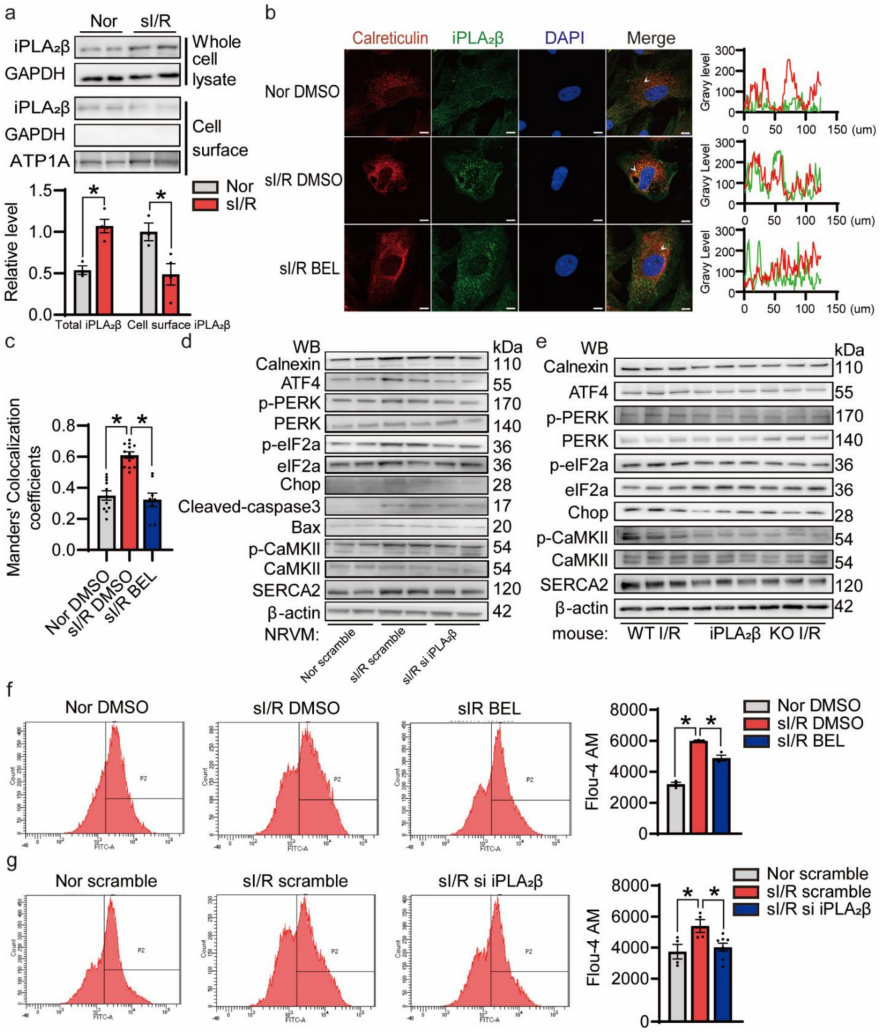

Figure 6. I/R promotes iPLA$_2$β translocate to the ER, leading to cardiomyocyte apoptosis induced by ER stress. (**a**) sI/R caused no significant increase in iPLA$_2$β on the cell surface membrane. NRVMs were subjected to sI/R and then placed on ice. EZ-link Sulfo-NHS-LC-Biotin was used to modify cell surface-localized proteins. After isolation of biotinylated surface proteins with neutravidin, immunoblotting was conducted to detect iPLA$_2$β. ATP1A was used as loading control of cell-surface-localized proteins. Quantification (below) revealed no increase in cardiomyocyte surface-localized iPLA$_2$β after sI/R. n = 3–4 for each group. (**b**) iPLA$_2$β was localized in the ER. iPLA$_2$β was detected by confocal immunofluorescence staining (green). ER was revealed by confocal immunofluorescence staining for calreticulin (red). The areas of interest are labeled with white arrows. The signaling intensity for both channels was scanned and recorded. Results are shown on the right. Scale bar = 20 μm. (**c**) Colocalization of iPLA$_2$β and ER was quantified by Mander's colocalization coefficients (MCCs). The comparison suggests that the inhibition of iPLA$_2$β significantly disrupts iPLA$_2$β and ER colocalization. n = 8–12 per group. (**d**) Knockdown of iPLA$_2$β relieved ER stress caused by I/R. Immunoblotting analysis was performed to detect the ER stress markers and Ca^{2+} -regulated related proteins. β-actin was used as a loading control. The protein levels of calnexin, ATF4, p-PERK, p-eIF2a, CHOP, cleaved-caspase3, Bax, p-CaMKII and SERCA2 were downregulated in the siiPLA$_2$β -transfected NRVMs. (**e**) Knockout of iPLA$_2$β relieved the ER stress caused by I/R. Immunoblotting analysis of ER stress markers and Ca^{2+}-regulated related proteins were performed. β-actin was used as a loading control. The protein levels of calnexin, ATF4, p-PERK, p-eIF2a, CHOP, p-CaMKII and SERCA2 were downregulated in the *Pla2g6* KO mouse heart tissues. (**f**) Inhibition of iPLA$_2$β by BEL reduced calcium overload upon sI/R. Intracellular Ca^{2+} was measured using 5 μM Fluo-4 AM. Mean fluorescence intensity indicates the concentration of intracellular Ca^{2+}. Quantification is shown on the right. n = 3 per group. (**g**) Knockdown of iPLA$_2$β reduced calcium overload during sI/R. Intracellular Ca^{2+} was measured using 5μM Fluo-4 AM. Mean fluorescence intensity indicates the concentration of intracellular Ca^{2+}. Quantification is shown on the right. n = 4–7 per group. Data are represented as the mean ± SEM. All experiments were independently replicated in triplicate. * $p < 0.05$.

4. Discussion

Coronary heart disease is caused by atherosclerotic lesions in the coronary arteries that narrow or block the lumen of the vessels, resulting in myocardial ischemia, hypoxia, or necrosis. Reports from the World Health Organization's website in 2017 show that cardiovascular disease (CVD) is the primary cause of death globally: more people die annually from CVD than from any other causes. Of these deaths, 85% are due to heart attack and stroke, with ischemic heart disease as the predominating one. The current development of PCI technology makes it possible to reduce the myocardial infarction area effectively and improve clinical outcomes. However, the mortality rate of patients with myocardial infarction still remains high. Studies have shown that even the restoration of blood flow to the ischemic myocardium cannot significantly reduce the infarct area, instead, further damage has been observed. This phenomenon is referred to as cardiac ischemia/reperfusion (I/R) injury. The pathological mechanism of cardiac I/R injury includes the accumulation of oxygen free radicals [33], calcium iron overload [34], energy metabolism failure [35], cell apoptosis [36] and other pathological factors. Cardiac I/R injury is a complex and multi-factorial pathological process that needs further investigations.

ER stress has been proven to be critical for the progression of cardiac diseases, including I/R [37–39]. In our study, we revealed the important effects of iPLA$_2$β on ER stress during myocardial I/R injury. The levels of iPLA$_2$β and ER stress markers were induced by sI/R injury, with a concomitant increase of apoptotic markers. Besides, inhibition of iPLA$_2$β in cardiomyocytes decreased cardiomyocyte death in response to sI/R injury via the ATF4/CHOP pathway. These results indicate that iPLA$_2$β increased upon I/R injury caused ER stress and further induced apoptosis. Moreover, iPLA$_2$β-deficient mice showed alleviated myocardial I/R injury. We also found that iPLA$_2$β participated in ER stress-induced apoptosis by translocating to the ER (Figure 7). Based on these, we propose that iPLA$_2$β is critical for the control of ER stress and cardiac function by its dynamic cellular localization.

iPLA$_2$β, which is also referred to as PLA$_2$ group VI and encoded by *PLA2G6*, contributes to the regulation of the concentration of phosphatidylcholine, a metabolite abundant in the cell membrane. iPLA$_2$β is also involved in multiple processes of phospholipid remodeling, arachidonic acid release [40], Fas receptor-mediated apoptosis [41,42], and transmembrane ion flux [43]. Mutations in *PLA2G6* have been proven to lead to mitochondrial dysfunction [44] and related neurological diseases [45–48], including Parkinson's disease 14 [49] and hereditary spastic paraplegia [50]. Intracellular localization of iPLA$_2$β is dynamic and tissue-specific [51,52]. Previous studies have shown that proinflammatory cytokines induce iPLA$_2$β upregulation-caused cell apoptosis by stimulation of ER stress in β-cells, an effect blocked by iPLA$_2$β inhibitor bromoenol lactone (BEL) [53].

iPLA$_2$β and cardiovascular function are closely related. iPLA$_2$β activation in the heart may result in both positive and negative effects [14,54,55]. The inhibition of iPLA$_2$ signaling pathway blocks the negative inotropic effect of HIV gp120 on cardiac myocytes [56], and activation of iPLA$_2$β has been reported to result in reduced conduction of arrhythmias caused by diabetic heart ischemia [57]. iPLA$_2$β also regulates calcium flow in various cells [58–61]. For example, iPLA$_2$ and its metabolite LPC play a key role in the control of endothelial store-operated Ca^{2+} entry and arterial tone [62].

It has been reported that the UPR is closely associated with lipid metabolism imbalance in the ER [63]. The UPR has been shown to be activated by changes in different lipids, which is independent of protein folding homeostasis in the ER lumen [64]. In this study, we established the heart I/R injury model in vivo and in vitro and observed that the activation of ER stress was accompanied by the upregulation of iPLA$_2$β. In view of the metabolic function of membrane phospholipids, we hypothesized that changes of iPLA$_2$β in the ER would lead to the disruption of ER function and thus cause ER stress. We confirmed that the increase of iPLA$_2$β in the ER lumen induced ER stress, caused calcium overload, and ultimately led to apoptosis. However, we did not determine the mechanism of iPLA$_2$β's translocation into ER under I/R, nor did we identify the ER protein that acts directly

with it. Further studies are required to answer these key questions. iPLA$_2$β is intensively studied in the field of the nervous system [65], and it has been reported that iPLA$_2$β's pathogenic causes are related to the structural and functional changes of the ER [66] and mitochondria [67]. Scoot et al. showed that iPLA$_2$β localizes in the mitochondria and affects the phospholipid metabolism of the mitochondrial membrane during myocardial I/R injury, which leads to the impairment of mitochondrial structure and function and consequently causes cardiomyocyte death [68]. Although many studies have confirmed the relationship between iPLA$_2$β and ER stress, our study contributes to the understanding of the connection between iPLA$_2$β and myocardial I/R injury. In addition, studies have reported that iPLA$_2$β is essential for maintaining basal ER homeostasis, suggesting that this enzyme performs different functions under pathological and physiological conditions.

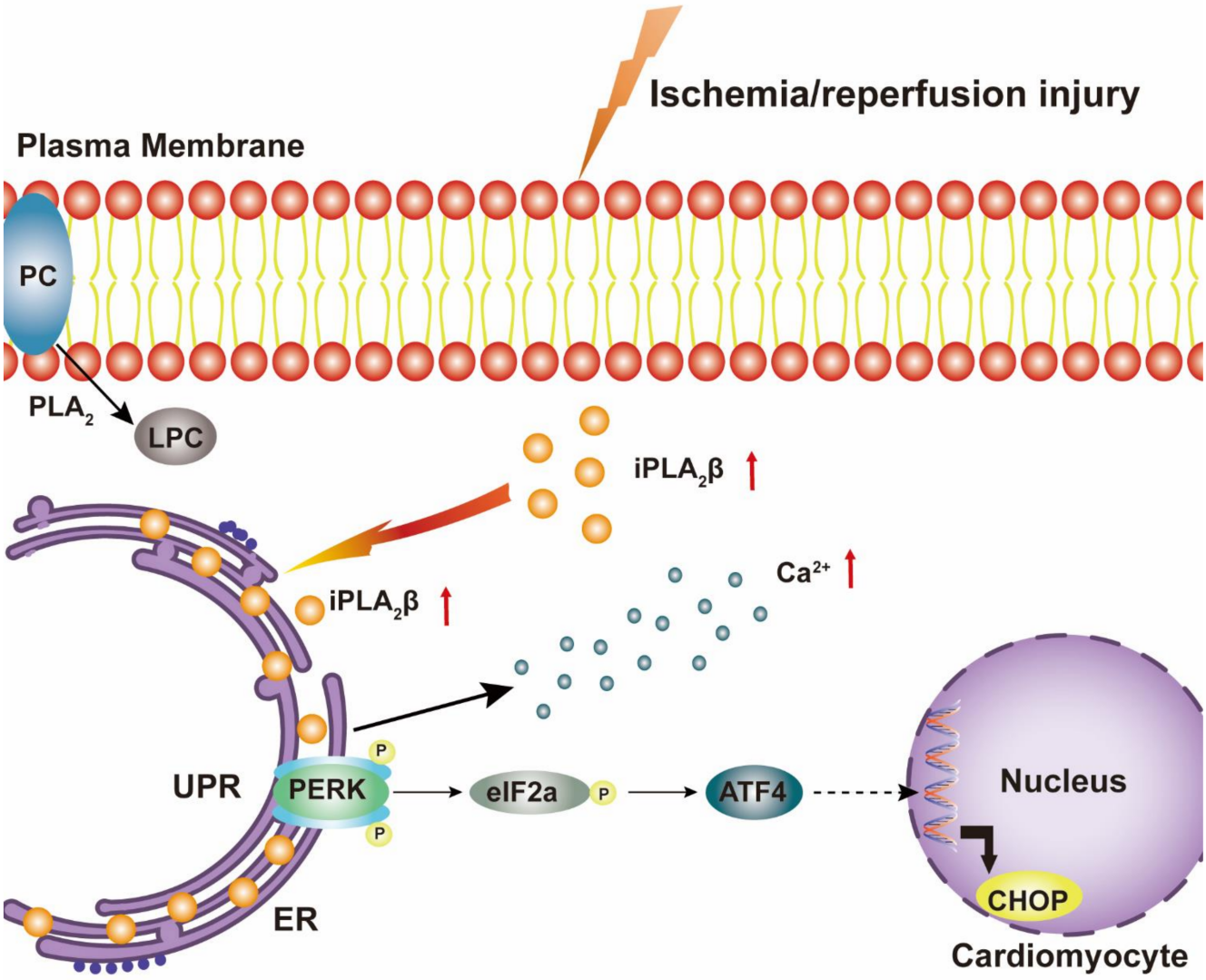

Figure 7. Illustration of the role of iPLA$_2$β on ER stress in cardiomyocyte upon I//R. PLA$_2$ expression is up-regulated in cardiomyocyte after I/R, which consequently leads to an increase of phosphatidylcholine (PC) metabolism. The generation of LPC is elevated and cardiomyocyte damage is augmented. The protein level of intracellular iPLA$_2$β, one of the PLA$_2$ enzymes, is upregulated. The increased iPLA$_2$β translocates to the ER and induces ER stress, which further leads to apoptosis through the PERK/ATF4/CHOP pathway. Additionally, iPLA$_2$β may also increase intracellular calcium flow in cardiomyocyte.

In summary, our study identified a key role of iPLA$_2$β in ER stress-induced apoptosis and in intracellular calcium homeostasis upon cardiac I/R. Inhibition of iPLA$_2$β reduces

myocardial I/R injury and preserves cardiac function. Therefore, inactivation of iPLA$_2\beta$ may serve as a potential therapeutic strategy for myocardial ischemia/reperfusion injury.

5. Limitation

We detected LPC concentration in the sera of patients with acute myocardial infarction by ELISA. Although previous reports have shown no significant difference in the detection results between ELISA and HPLC methods [69,70], it is undeniable that HPLC is more accurate, stable and specific than ELISA [71]. LPCs are a class of metabolites derived from phosphatidylcholines, which are composed of a variety of species [72]. Due to the unavailability of HPLC, we could not detect and analyze the various LPC components.

The neonatal cardiomyocytes were chosen for in vitro experiments in our study. There are some limitations in using neonatal cardiomyocytes as a model system. First, the phenotypic immaturity of neonatal cardiomyocytes limits the full translation of the findings to the in vivo conditions, for example, metabolic characteristics of neonatal cells are different from those in adult cardiomyocytes [73]. Secondly, the lack of extracellular matrix in the culture system may alter the behavior of these cells, resulting in a certain discrepancy between in vitro and in vivo findings [74].

Supplementary Materials: The following materials are available online at https://www.mdpi.com/article/10.3390/cells10061446/s1, Supplement Figure S1. Simulated ischemia/reperfusion (sI/R) injury-triggered ER stress in NRVMs. Supplement Figure S2. Analysis of *Pla2g6*$^{-/-}$ mice and wild-type mice. Supplement Figure S3. No significant difference in the expression of CHOP at the basal level between WT and KO mice. Supplement Figure S4. The inhibition of iPLA$_2\beta$ in vitro and in vivo decreased ER stress as well as subsequent apoptosis. Supplement Figure S5. sI/R led to NRVM apoptosis induced by ER stress but not through the ATF6 and p-IRE1α pathways.

Author Contributions: Conceptualization, T.J., X.B. and G.F.; Data curation, T.J.; Formal analysis, T.J. and J.L.; Funding acquisition, X.L., W.Z. and G.F.; Investigation, G.F.; Methodology, T.J., J.L., Y.G., S.H. and J.C. (Jiaweng Chen); Resources, W.Z. and M.W.; Software, J.L., Y.G. and Q.L.; Supervision, M.W.; Validation, W.Z.; Visualization, T.J.; Writing—original draft, T.J.; Writing—review and editing, T.J., X.B. and J.C. (Jiaqi Chen). All authors have read and agreed to the published version of the manuscript.

Funding: This study was supported by the National Natural Science Foundation of China (82070359); Natural Key Research and Development Project of Zhejiang Province, China (2018C03015); National Key Research and Development Program of China (2016YFC1102203); Natural Science Foundation of Zhejiang Province (82070408); National Natural Science Foundation of China (81900232 to X.B. and 81800706 to X.L.); Natural Science Foundation of Zhejiang Province (LQ19H020011 to X.B.); Chinese Postdoctoral Science Foundation (2019M652118 to X.B.); Natural Science Funds of Zhejiang Province, China (Project Nos. LY20H020004); Medical and Health Science Program of Zhejiang Province (No. 2018278178); National Natural Science Foundation of China (No. 82000404) and a grant from the Natural Science Funds of Zhejiang Province, China (Project No. LQ21H020003). The funders did not have any role in study design, data collection, data analysis, interpretation or writing of the report.

Institutional Review Board Statement: The study was conducted according to the guidelines of the Declaration of Helsinki and approved by the Medical Ethics Committee of Run Run Shaw Hospital affiliated with Zhejiang University (20200210-113) and the Animal Welfare Ethics Committee of Run Run Shaw Hospital affiliated Zhejiang University (SRRSH202002233).

Informed Consent Statement: Informed consent was obtained from all subjects involved in the study.

Data Availability Statement: Data presented in the article are available by request to first author, Tingting Jin (11818361@zju.edu.cn).

Acknowledgments: The authors are grateful for the technical support provided by the Core Facilities, Zhejiang University School of Medicine.

Conflicts of Interest: The authors declare no conflict of interest. The funders had no role in the design of the study; in the collection, analyses, or interpretation of data; in the writing of the manuscript, or in the decision to publish the results.

References

1. Virani, S.S.; Alonso, A.; Benjamin, E.J.; Bittencourt, M.S.; Callaway, C.W.; Carson, A.P. Heart Disease and Stroke Statistics-2020 Update: A Report From the American Heart Association. *Circulation* **2020**, *141*, e139–e596. [CrossRef]
2. Hausenloy, D.J.; Yellon, D.M. Myocardial ischemia-reperfusion injury: A neglected therapeutic target. *J. Clin. Investig.* **2013**, *123*, 92–100. [CrossRef]
3. Hausenloy, D.J.; Chilian, W.; Crea, F.; Davidson, S.M.; Ferdinandy, P.; Garcia-Dorado, D.; Van Royen, N.; Schulz, R.; Heusch, G. The coronary circulation in acute myocardial ischaemia/reperfusion injury: A target for cardioprotection. *Cardiovasc. Res.* **2019**, *115*, 1143–1155. [CrossRef]
4. Yellon, D.; Hausenloy, D.J. Myocardial Reperfusion Injury. *N. Engl. J. Med.* **2007**, *357*, 1121–1135. [CrossRef]
5. Schröder, M.; Kaufman, R.J. The Mammalian Unfolded Protein Response. *Annu. Rev. Biochem.* **2005**, *74*, 739–789. [CrossRef]
6. Xu, C.; Bailly-Maitre, B.; Reed, J.C. Endoplasmic reticulum stress: Cell life and death decisions. *J. Clin. Investig.* **2005**, *115*, 2656–2664. [CrossRef]
7. Ron, D.; Walter, P. Signal integration in the endoplasmic reticulum unfolded protein response. *Nat. Rev. Mol. Cell Biol.* **2007**, *8*, 519–529. [CrossRef] [PubMed]
8. Wang, Z.V.; Deng, Y.; Gao, N.; Pedrozo, Z.; Li, D.L.; Morales, C.R.; Criollo, A.; Luo, X.; Tan, W.; Jiang, N.; et al. Spliced X-Box Binding Protein 1 Couples the Unfolded Protein Response to Hexosamine Biosynthetic Pathway. *Cell* **2014**, *156*, 1179–1192. [CrossRef]
9. Meyer, B.A.; Doroudgar, S. ER Stress-Induced Secretion of Proteins and Their Extracellular Functions in the Heart. *Cells* **2020**, *9*, 2066. [CrossRef] [PubMed]
10. Arnsdorf, M.F.; Sawicki, G.J. The effects of lysophosphatidylcholine, a toxic metabolite of ischemia, on the components of cardiac excitability in sheep Purkinje fibers. *Circ. Res.* **1981**, *49*, 16–30. [CrossRef] [PubMed]
11. Lawrence, K.M.; Scarabelli, T.M.; Turtle, L.; Chanalaris, A.; Townsend, P.A.; Carroll, C.J.; Hubank, M.; Stephanou, A.; Knight, R.A.; Latchman, D.S. Urocortin protects cardiac myocytes from ischemia/reperfusion injury by attenuating calcium insensitive phospholipase A 2 gene expression. *FASEB J.* **2003**, *17*, 2313–2315. [CrossRef]
12. Shinzawa, K.; Tsujimoto, Y. PLA2 activity is required for nuclear shrinkage in caspase-independent cell death. *J. Cell Biol.* **2003**, *163*, 1219–1230. [CrossRef]
13. Ghosh, M.; Tucker, D.E.; Burchett, S.A.; Leslie, C.C. Properties of the Group IV phospholipase A2 family. *Prog. Lipid Res.* **2006**, *45*, 487–510. [CrossRef]
14. Lei, X.; Bone, R.N.; Ali, T.; Zhang, S.; Bohrer, A.; Tse, H.M.; Bidasee, K.R.; Ramanadham, S. Evidence of Contribution of iPLA2β-Mediated Events During Islet β-Cell Apoptosis Due to Proinflammatory Cytokines Suggests a Role for iPLA2β in T1D Development. *Endocrinology* **2014**, *155*, 3352–3364. [CrossRef] [PubMed]
15. Ramanadham, S.; Ali, T.; Ashley, J.; Bone, R.N.; Hancock, W.D.; Lei, X. Calcium-independent phospholipases A2 and their roles in biological processes and diseases. *J. Lipid Res.* **2015**, *56*, 1643–1668. [CrossRef] [PubMed]
16. Song, H.; Bao, S.; Lei, X.; Jin, C.; Zhang, S.; Turk, J. Evidence for proteolytic processing and stimulated organelle redistribution of iPLA(2)beta. *Biochim. Biophys. Acta* **2010**, *1801*, 547–558. [CrossRef] [PubMed]
17. Malley, K.R.; Koroleva, O.; Miller, I.; Sanishvili, R.; Jenkins, C.M.; Gross, R.W.; Korolev, S. The structure of iPLA2β reveals dimeric active sites and suggests mechanisms of regulation and localization. *Nat. Commun.* **2018**, *9*, 1–11. [CrossRef] [PubMed]
18. Fang, S.-J.; Li, P.-Y.; Wang, C.; Xin, Y.; Lu, W.-W.; Zhang, X.-X.; Zuo, S.; Ma, C.-S.; Tang, C.-S.; Nie, S.-P.; et al. Inhibition of endoplasmic reticulum stress by neuregulin-1 protects against myocardial ischemia/reperfusion injury. *Peptides* **2017**, *88*, 196–207. [CrossRef]
19. Ngoh, G.A.; Facundo, H.T.; Hamid, T.; Dillmann, W.; Zachara, N.E.; Jones, S.P. Unique Hexosaminidase Reduces Metabolic Survival Signal and Sensitizes Cardiac Myocytes to Hypoxia/Reoxygenation Injury. *Circ. Res.* **2009**, *104*, 41–49. [CrossRef]
20. Wang, J.X.; Zhang, X.J.; Li, Q.; Wang, K.; Wang, Y.; Jiao, J.Q. MicroRNA-103/107 Regulate Programmed Necrosis and Myocardial Ischemia/Reperfusion Injury Through Targeting FADD. *Circ. Res.* **2015**, *117*, 352–363. [CrossRef]
21. Zinchuk, V.; Grossenbacher-Zinchuk, O. Quantitative colocalization analysis of confocal fluorescence microscopy images. *Curr. Protocols Cell Biol.* **2008**, *39*, 4–19. [CrossRef]
22. Sobel, B.E.; Corr, P.B.; Robison, A.K.; Goldstein, R.A.; Witkowski, F.X.; Klein, M.S. Accumulation of lysophosphoglycerides with arrhythmogenic properties in ischemic myocardium. *J. Clin. Investig.* **1978**, *62*, 546–553. [CrossRef] [PubMed]
23. Corr, P.B.; Gross, R.W.E.; Sobel, B. Amphipathic metabolites and membrane dysfunction in ischemic myocardium. *Circ. Res.* **1984**, *55*, 135–154. [CrossRef] [PubMed]
24. Zhang, R.; Bai, N.; So, J.; Laher, I.; MacLeod, K.; Rodrigues, B. The ischemic metabolite lysophosphatidylcholine increases rat coronary arterial tone by endothelium-dependent mechanisms. *J. Mol. Cell. Cardiol.* **2009**, *47*, 112–120. [CrossRef]
25. Anwar, K.; Voloshyna, I.; Littlefield, M.J.; Carsons, S.E.; Wirkowski, P.A.; Jaber, N.L.; Sohn, A.; Eapen, S.; Reiss, A.B. COX-2 Inhibition and Inhibition of Cytosolic Phospholipase A2 Increase CD36 Expression and Foam Cell Formation in THP-1 Cells. *Lipids* **2010**, *46*, 131–142. [CrossRef] [PubMed]
26. Rosenson, R.S. Future Role for Selective Phospholipase A2 Inhibitors in the Prevention of Atherosclerotic Cardiovascular Disease. *Cardiovasc. Drugs Ther.* **2009**, *23*, 93–101. [CrossRef]

27. Mallat, Z.; Steg, P.G.; Benessiano, J.; Tanguy, M.-L.; Fox, K.A.; Collet, J.-P.; Dabbous, O.H.; Henry, P.; Carruthers, K.F.; Dauphin, A.; et al. Circulating Secretory Phospholipase A2 Activity Predicts Recurrent Events in Patients With Severe Acute Coronary Syndromes. *J. Am. Coll. Cardiol.* **2005**, *46*, 1249–1257. [CrossRef] [PubMed]
28. Zalewski, A.; Macphee, C. Role of Lipoprotein-Associated Phospholipase A_2 in Atherosclerosis. *Arterioscler. Thromb. Vasc. Biol.* **2005**, *25*, 923–931. [CrossRef]
29. Mancuso, D.J.; Abendschein, D.R.; Jenkins, C.M.; Han, X.; Saffitz, J.E.; Schuessler, R.B.; Gross, R.W. Cardiac ischemia activates calcium-independent phospholipase A(2)beta, precipitating ventricular tachyarrhythmias in transgenic mice—Rescue of the lethal electrophysiologic phenotype by mechanism-based inhibition. *J. Biol. Chem.* **2003**, *278*, 22231–22236. [CrossRef]
30. Moon, S.H.; Mancuso, D.J.; Sims, H.F.; Liu, X.; Nguyen, A.L.; Yang, K.; Guan, S.; Dilthey, B.G.; Jenkins, C.M.; Weinheimer, C.J.; et al. Cardiac Myocyte-specific Knock-out of Calcium-independent Phospholipase A2γ (iPLA2γ) Decreases Oxidized Fatty Acids during Ischemia/Reperfusion and Reduces Infarct Size. *J. Biol. Chem.* **2016**, *291*, 19687–19700. [CrossRef]
31. Fuentes, L.; Pérez, R.; Nieto, M.L.; Balsinde, J.; Balboa, M.A. Bromoenol Lactone Promotes Cell Death by a Mechanism Involving Phosphatidate Phosphohydrolase-1 Rather than Calcium-independent Phospholipase A2. *J. Biol. Chem.* **2003**, *278*, 44683–44690. [CrossRef]
32. Whelan, R.S.; Kaplinskiy, V.; Kitsis, R.N. Cell Death in the Pathogenesis of Heart Disease: Mechanisms and Significance. *Annu. Rev. Physiol.* **2010**, *72*, 19–44. [CrossRef] [PubMed]
33. Li, H.; Xia, Z.; Chen, Y.; Qi, D.; Zheng, H. Mechanism and Therapies of Oxidative Stress-Mediated Cell Death in Ischemia Reperfusion Injury. *Oxidative Med. Cell. Longev.* **2018**, *2018*, 1–2. [CrossRef] [PubMed]
34. Aghaei, M.; Motallebnezhad, M.; Ghorghanlu, S.; Jabbari, A.; Enayati, A.; Rajaei, M.; Pourabouk, M.; Moradi, A.; Alizadeh, A.M.; Khori, V. Targeting autophagy in cardiac ischemia/reperfusion injury: A novel therapeutic strategy. *J. Cell. Physiol.* **2019**, *234*, 16768–16778. [CrossRef]
35. Cheng, Y.; Xia, Z.; Han, Y.; Rong, J. Plant Natural Product Formononetin Protects Rat Cardiomyocyte H9c2 Cells against Oxygen Glucose Deprivation and Reoxygenation via Inhibiting ROS Formation and Promoting GSK-3βPhosphorylation. *Oxidative Med. Cell. Longev.* **2016**, *2016*, 1–11. [CrossRef]
36. Dong, Y.; Chen, H.; Gao, J.; Liu, Y.; Li, J.; Wang, J. Molecular machinery and interplay of apoptosis and autophagy in coronary heart disease. *J. Mol. Cell. Cardiol.* **2019**, *136*, 27–41. [CrossRef]
37. Minamino, T.; Komuro, I.; Kitakaze, M. Endoplasmic Reticulum Stress As a Therapeutic Target in Cardiovascular Disease. *Circ. Res.* **2010**, *107*, 1071–1082. [CrossRef]
38. Bi, X.; Zhang, G.; Wang, X.; Nguyen, C.Y.; May, H.; Li, X.; Al-Hashimi, A.A.; Austin, R.C.; Gillette, T.G.; Fu, G.S.; et al. Endoplasmic Reticulum Chaperone GRP78 Protects Heart From Ischemia/Reperfusion Injury Through Akt Activation. *Circ. Res.* **2018**, *122*, 1545–1554. [CrossRef] [PubMed]
39. Zhu, P.; Hu, S.; Jin, Q.; Li, D.; Tian, F.; Toan, S.; Li, Y.; Zhou, H.; Chen, Y. Ripk3 promotes ER stress-induced necroptosis in cardiac IR injury: A mechanism involving calcium overload/XO/ROS/mPTP pathway. *Redox Biol.* **2018**, *16*, 157–168. [CrossRef]
40. Bao, S.; Li, Y.; Lei, X.; Wohltmann, M.; Jin, W.; Bohrer, A.; Semenkovich, C.F.; Ramanadham, S.; Tabas, I.; Turk, J. Attenuated Free Cholesterol Loading-induced Apoptosis but Preserved Phospholipid Composition of Peritoneal Macrophages from Mice That Do Not Express Group VIA Phospholipase A2. *J. Biol. Chem.* **2007**, *282*, 27100–27114. [CrossRef]
41. Atsumi, G.-I.; Tajima, M.; Hadano, A.; Nakatani, Y.; Murakami, M.; Kudo, I. Fas-induced Arachidonic Acid Release Is Mediated by Ca2+-independent Phospholipase A2 but Not Cytosolic Phospholipase A2, Which Undergoes Proteolytic Inactivation. *J. Biol. Chem.* **1998**, *273*, 13870–13877. [CrossRef] [PubMed]
42. Sun, W.-Y.; Tyurin, V.A.; Mikulska-Ruminska, K.; Shrivastava, I.H.; Anthonymuthu, T.S.; Zhai, Y.-J.; Pan, M.-H.; Gong, H.-B.; Lu, D.-H.; Sun, J.; et al. Phospholipase iPLA2β averts ferroptosis by eliminating a redox lipid death signal. *Nat. Chem. Biol.* **2021**, 1–12. [CrossRef]
43. Abeele, F.V.; Zholos, A.; Bidaux, G.; Shuba, Y.; Thebault, S.; Beck, B.; Flourakis, M.; Panchin, Y.; Skryma, R.; Prevarskaya, N. Ca2+-independent phospholipase A2-dependent gating of TRPM8 by lysophospholipids. *J. Biol. Chem.* **2006**, *281*, 40174–40182. [CrossRef] [PubMed]
44. Beck, G.; Sugiura, Y.; Shinzawa, K.; Kato, S.; Setou, M.; Tsujimoto, Y.; Sakoda, S.; Sumi-Akamaru, H. Neuroaxonal Dystrophy in Calcium-Independent Phospholipase A2β Deficiency Results from Insufficient Remodeling and Degeneration of Mitochondrial and Presynaptic Membranes. *J. Neurosci.* **2011**, *31*, 11411–11420. [CrossRef]
45. Meyer, E.; Kurian, M.A.; Hayflick, S.J. Neurodegeneration with Brain Iron Accumulation: Genetic Diversity and Pathophysiological Mechanisms. *Annu. Rev. Genom. Hum. Genet.* **2015**, *16*, 257–279. [CrossRef]
46. Morgan, N.V.; Westaway, S.K.; Morton, J.E.; Gregory, A.; Gissen, P.; Sonek, S. PLA2G6, encoding a phospholipase A2, is mutated in neurodegenerative disorders with high brain iron. *Nat. Genet.* **2006**, *38*, 752–754. [CrossRef]
47. Kruer, M.C.; Paisán-Ruiz, C.; Boddaert, N.; Yoon, M.Y.; Hama, H.; Ms, A.G.; Malandrini, A.; Woltjer, R.L.; Munnich, A.; Gobin, S.; et al. Defective FA2H leads to a novel form of neurodegeneration with brain iron accumulation (NBIA). *Ann. Neurol.* **2010**, *68*, 611–618. [CrossRef] [PubMed]
48. Schneider, S.A.; Hardy, J.; Bhatia, K.P. Syndromes of neurodegeneration with brain iron accumulation (NBIA): An update on clinical presentations, histological and genetic underpinnings, and treatment considerations. *Mov. Disord.* **2011**, *27*, 42–53. [CrossRef] [PubMed]

49. Zhou, Q.; Yen, A.; Rymarczyk, G.; Asai, H.; Trengrove, C.; Aziz, N.; Kirber, M.T.; Mostoslavsky, G.; Ikezu, T.; Wolozin, B.; et al. Impairment of PARK14-dependent Ca2+ signalling is a novel determinant of Parkinson's disease. *Nat. Commun.* **2016**, *7*, 10332. [CrossRef] [PubMed]
50. Guidubaldi, A.; Piano, C.; Santorelli, F.M.; Silvestri, G.; Petracca, M.; Tessa, A.; Bentivoglio, A.R. Novel mutations in SPG11 cause hereditary spastic paraplegia associated with early-onset levodopa-responsive Parkinsonism. *Mov. Disord.* **2011**, *26*, 553–556. [CrossRef]
51. Bao, S.; Jin, C.; Zhang, S.; Turk, J.; Ma, Z.; Ramanadham, S. Beta-cell calcium-independent group VIA phospholipase A(2) (iPLA(2)beta): Tracking iPLA(2)beta movements in response to stimulation with insulin secretagogues in INS-1 cells. *Diabetes* **2004**, *53*, S186–S189. [CrossRef]
52. Seleznev, K.; Zhao, C.; Zhang, X.H.; Song, K.; Ma, Z.A. Calcium-independent phospholipase A2 localizes in and protects mitochondria during apoptotic induction by staurosporine. *J. Biol. Chem.* **2006**, *281*, 22275–22288. [CrossRef]
53. Ramanadham, S.; Song, H.; Bao, S.; Hsu, F.F.; Zhang, S.; Ma, Z.; Jin, C.; Turk, J. Islet complex lipids: Involvement in the actions of group VIA calcium-independent phospholipase A(2) in beta-cells. *Diabetes* **2004**, *53*, S179–S185. [CrossRef] [PubMed]
54. Andersen, A.-D.; Poulsen, K.A.; Lambert, I.H.; Pedersen, S.F. HL-1 mouse cardiomyocyte injury and death after simulated ischemia and reperfusion: Roles of pH, Ca2+-independent phospholipase A2, and Na+/H+ exchange. *Am. J. Physiol. Physiol.* **2009**, *296*, C1227–C1242. [CrossRef] [PubMed]
55. Sharma, J.; Blasé, J.R.; Hoft, D.F.; Marentette, J.O.; Turk, J.; McHowat, J. Mice with Genetic Deletion of Group VIA Phospholipase A2β Exhibit Impaired Macrophage Function and Increased Parasite Load in Trypanosoma cruzi-Induced Myocarditis. *Infect. Immun.* **2016**, *84*, 1137–1142. [CrossRef]
56. Kan, H.; Xie, Z.; Finkel, M.S. iPLA2 inhibitor blocks negative inotropic effect of HIV gp120 on cardiac myocytes. *J. Mol. Cell. Cardiol.* **2006**, *40*, 131–137. [CrossRef]
57. Su, X.; Han, X.; Mancuso, D.J.; Abendschein, A.D.R.; Gross, R.W. Accumulation of Long-Chain Acylcarnitine and 3-Hydroxy Acylcarnitine Molecular Species in Diabetic Myocardium: Identification of Alterations in Mitochondrial Fatty Acid Processing in Diabetic Myocardium by Shotgun Lipidomics†. *Biochemistry* **2005**, *44*, 5234–5245. [CrossRef]
58. Smani, T.; Zakharov, S.I.; Leno, E.; Csutora, P.; Trepakova, E.S.; Bolotina, V.M. Ca2+-independent Phospholipase A2 Is a Novel Determinant of Store-operated Ca2+ Entry. *J. Biol. Chem.* **2003**, *278*, 11909–11915. [CrossRef]
59. Singaravelu, K.; Lohr, C.; Deitmer, J.W. Regulation of Store-Operated Calcium Entry by Calcium-Independent Phospholipase A2 in Rat Cerebellar Astrocytes. *J. Neurosci.* **2006**, *26*, 9579–9592. [CrossRef]
60. Boittin, F.-X.; Petermann, O.; Hirn, C.; Mittaud, P.; Dorchies, O.M.; Roulet, E.; Ruegg, U. Ca2+-independent phospholipase A2 enhances store-operated Ca2+ entry in dystrophic skeletal muscle fibers. *J. Cell Sci.* **2006**, *119*, 3733–3742. [CrossRef]
61. Ross, K.; Whitaker, M.; Reynolds, N.J. Agonist-induced calcium entry correlates with STIM1 translocation. *J. Cell. Physiol.* **2007**, *211*, 569–576. [CrossRef] [PubMed]
62. Boittin, F.-X.; Gribi, F.; Serir, K.; Bény, J.-L. Ca2+-independent PLA2 controls endothelial store-operated Ca2+ entry and vascular tone in intact aorta. *Am. J. Physiol. Circ. Physiol.* **2008**, *295*, H2466–H2474. [CrossRef]
63. Ming, Y.; Zhu, X.; Tuma-Kellner, S.; Ganzha, A.; Liebisch, G.; Gan-Schreier, H.; Chamulitrat, W. iPla2β Deficiency Suppresses Hepatic ER UPR, Fxr, and Phospholipids in Mice Fed with MCD Diet, Resulting in Exacerbated Hepatic Bile Acids and Biliary Cell Proliferation. *Cells* **2019**, *8*, 879. [CrossRef] [PubMed]
64. Fun, X.H.; Thibault, G. Lipid bilayer stress and proteotoxic stress-induced unfolded protein response deploy divergent transcriptional and non-transcriptional programmes. *Biochim. Biophys. Acta BBA Mol. Cell Biol. Lipids* **2020**, *1865*, 158449. [CrossRef] [PubMed]
65. Chung, C.Y.; Shi, Y.; Surendranath, A.R.; Jalal, N.; Pathak, J.L.; Subramaniyam, S. Role of Calcium-Independent Phospholipase A2 VIA in Mediating Neurological Disorder and Cancer. *Trans. Tianjin Univ.* **2017**, *23*, 1–10. [CrossRef]
66. Mori, A.; Hatano, T.; Inoshita, T.; Shiba-Fukushima, K.; Koinuma, T.; Meng, H.; Kubo, S.-I.; Spratt, S.; Cui, C.; Yamashita, C.; et al. Parkinson's disease-associated iPLA2-VIA/PLA2G6 regulates neuronal functions and α-synuclein stability through membrane remodeling. *Proc. Natl. Acad. Sci. USA* **2019**, *116*, 20689–20699. [CrossRef] [PubMed]
67. Kinghorn, K.J.; Castillo-Quan, J.I.; Bartolome, F.; Angelova, P.R.; Li, L.; Pope, S.; Cochemé, H.M.; Khan, S.; Asghari, S.; Bhatia, K.P.; et al. Loss ofPLA2G6leads to elevated mitochondrial lipid peroxidation and mitochondrial dysfunction. *Brain* **2015**, *138*, 1801–1816. [CrossRef] [PubMed]
68. Williams, S.D.; Gottlieb, R.A. Inhibition of mitochondrial calcium-independent phospholipase A2 (iPLA2) attenuates mitochondrial phospholipid loss and is cardioprotective. *Biochem. J.* **2002**, *362*, 23–32. [CrossRef]
69. Dohnal, V.; Dvořák, V.; Malíř, F.; Ostrý, V.; Roubal, T. A comparison of ELISA and HPLC methods for determination of ochratoxin A in human blood serum in the Czech Republic. *Food Chem. Toxicol.* **2013**, *62*, 427–431. [CrossRef]
70. Beyene, A.M.; Du, X.; Schrunk, D.E.; Ensley, S.; Rumbeiha, W.K. High-performance liquid chromatography and Enzyme-Linked Immunosorbent Assay techniques for detection and quantification of aflatoxin B1 in feed samples: A comparative study. *BMC Res. Notes* **2019**, *12*, 1–6. [CrossRef]
71. Omar, S.S.; Haddad, M.A.; Parisi, S. Validation of HPLC and Enzyme-Linked Immunosorbent Assay (ELISA) Techniques for Detection and Quantification of Aflatoxins in Different Food Samples. *Foods* **2020**, *9*, 661. [CrossRef]
72. Huang, Q.; Lei, H.; Dong, M.; Tang, H.; Wang, Y. Quantitative analysis of 10 classes of phospholipids by ultrahigh-performance liquid chromatography tandem triple-quadrupole mass spectrometry. *Analyst* **2019**, *144*, 3980–3987. [CrossRef] [PubMed]

73. Stanley, W.C.; Recchia, F.A.; Lopaschuk, G.D. Myocardial Substrate Metabolism in the Normal and Failing Heart. *Physiol. Rev.* **2005**, *85*, 1093–1129. [CrossRef]
74. Ruwhof, C.; van der Laarse, A. Mechanical stress-induced cardiac hypertrophy: Mechanisms and signal transduction pathways. *Cardiovasc. Res.* **2000**, *47*, 23–37. [CrossRef]